Journal of the European Ceramic Society **18** (1998) 1107–1114

PII: S0955-2219(97)00191-X
0955-2219/98/$19.00 + 0.00

Microstructure and Mechanical Properties of Mullite Ceramics Containing Rodlike Particles

Jiahong Meng, Shu Cai, Zhengfang Yang, Qiming Yuan and Yuru Chen

Department of Materials Science and Engineering, Tianjin University, Tianjin 300072, People's Republic of China

(Received 23 June 1997; revised version received 12 September 1997; accepted 22 October 1997)

Abstract

Mullite/mullite (rodlike) microstructure which has whisker-like grains with high aspect ratios within a fine grain matrix was obtained by adding AlF_3 into mullite precursor and heat-treated at 1150°C in air-tight condition and then sintering at high temperature. The grain growth conditions of rodlike mullite were existence of high Al_2O_3/SiO_2 ratio grains and existence of liquid phase. The fracture toughness increased by the growth of rodlike mullite particles and at the same time the flexural strength did not decrease. © 1998 Elsevier Science Limited. All rights reserved

1 Introduction

Mullite ceramics have many desirable and usable properties, such as excellent high-temperature strength and creep resistance, good thermal and chemical stability, low thermal-expansion coefficient, low true density and good dielectric properties.[1–6] But the mechanical properties of mullite ceramics at room temperature are relatively low, especially fracture toughness which is just 2–3 $\mathrm{MPa\,m^{1/2}}$.[2] Many methods have been used to improve the fracture toughness of mullite and notable progresses have been achieved. Among these methods, adding second phase (such as particles, whiskers, fibers, etc.) is extensively used. In most cases, second phases can be incorporated into the matrix by mixing them mechanically with the raw powders before sintering. Nevertheless, these improvements of fracture toughness may occur at the expanse of strength when the second phase acts as a flaw initiation site. In addition, second phase may also inhibit densification, making it necessary to hot-press or HIP to obtain high densities. For some ceramics, by adjusting fabrication process or heat-treatment process, by way of in-situ formation of a second phase which has a highly anisotropy growth habit, a toughened ceramic composite can be obtained without sintering difficulties.[7,8] The effect of the developing elongated grains on toughening was first demonstrated in silicon nitride ceramics, which improved the fracture toughness successfully.[9–11]

Microstructures of mullite ceramics differ greatly in their Al_2O_3/SiO_2 ratios. For silica-rich mullite, the grains tend to be circular particles, and aluminum-rich samples, equiaxed particles appear.[12,13] The composition-controlled microstructure of mullite ceramics directly controls the mechanical properties of the materials. The interlocked network of prismatic mullite crystals occurring in low-Al_2O_3 mullite composition produces favorable mechanical strength values by mullite–mullite (self-)reinforcement up to relatively high temperature (<1200°C),[14] so the development of mullite/mullite (rodlike) structure may be very useful for mullite ceramics used in mechanical field. In this paper, a new processing route was designed to obtain mullite ceramic with self-reinforcement microstructure by using the technique of synthesizing mullite whiskers through vapor-phase reaction.

2 Experimental Procedure

2.1 Microstructure designing

For prismatic crystals in natural mullite, the elongated direction is [001].[15] Crystal habit of mullite whisker prepared by vapor-phase reaction is also in [001].[16] Thus a suitable amount of nuclei of mullite whiskers produced in the green compacts could be used as the growth centers for rodlike particles, and rodlike particles can be developed after high temperature sintering. In this experiment, the processing route was designed as following (Fig. 1).

A small amount of AlF_3 was added into mullite precursor and the green compacts were heat-treated

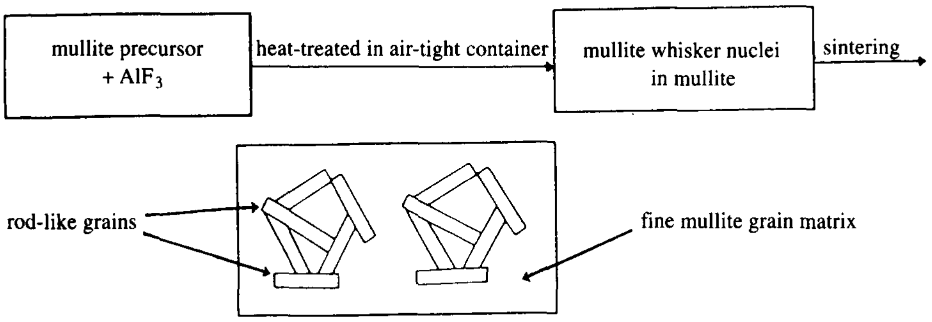

Fig. 1. Designing route of mullite microstructure.

in an airtight container at suitable temperature, in this process the mullite whisker nuclei can be produced. Finally the samples were sintered to high density at higher temperature.

2.2 Raw materials and sample preparing

The preparation method of mullite precursor was hydrolysis-precipitation.[17] The starting materials were aluminum chloride 6-hydrate ($AlCl_3{\cdot}6H_2O$) and tetraethyl orthosilicate (TEOS).SiO_2-rich [$Al_2O_3/SiO_2 = 68/32$ (wt/wt)] composition was selected. The mullite precursor xerogels were calcined at 1000 and 1250°C, respectively. The samples were as follows:

1. 1000°C calcined mullite precursor +0·5 wt% AlF_3;
2. 85% 1250°C calcined mullite precursor +15% 1000°C calcined mullite precursor +0·5 wt% AlF_3;
3. 1000°C calcined mullite precursor.

The mixed powders of mullite precursor and AlF_3 were uniaxialy pressed at 50 MPa followed by cold-isostatic pressing at 200 MPa. The green compacts were heat-treated at a range of 1100–1450°C in an airtight container, and then sintered at 1500–1600°C for 4 h in air.

An airtight ZTM container was prepared by polishing the contact parts of a cover plate and the rim of a crucible, a process described by Okada and Otsuka.[18] In order to guarantee airtightness, two sets of crucibles were used.

2.3 Experimental methods

Differential thermal analysis (DTA) was performed with a computer-controlled apparatus. Eighty milligrams of the precursor powders and the reference material (fired α-Al_2O_3), respectively, were heated in a Pt crucible with a constant heating rate of $10°C\,min^{-1}$. DTA was carried out in N_2 atmosphere. The crystallization behavior of the mullite processor was observed by X-ray diffraction (XRD) using Co K_α radiation and the X-ray diffraction patterns of sintered samples were obtained using Cu K_α radiation. The bulk densities of green compacts were measured by the geometrical method by exactly measuring the weight and dimension of samples. Sintered densities were determined using the Archimedes method with distilled water. The relative density was calculated from the theoretical density of mullite (68/32), $3{\cdot}12\,g\,cm^{-3}$. The samples were polished and thermally etched (50°C lower than their sintering temperatures) for 1 h and were examined using scanning electron microscopy (Model S-500) equipped with energy dispersive X-ray analysis (EDX).

TEM observations were performed on a JEM-200CXII (equipped with EDX) transmission electron microscopy at 200 KV. Thin foils of samples for TEM were prepared by dimple grinding and argon-ion thinning. The foils were coated with carbon films to avoid charging effects.

The strength was measured by three-point bending with span of 20 mm. The fracture toughness was determined by the single-edge notched beam method. Every strength value reported was the average of at least five samples and every fracture toughness value was obtained from at least three bars.

3 Results and Discussion

3.1 The properties of mullite precursor

The curve of differential thermal analysis of mullite precursor is shown in Fig. 2. There is not any transformation exothermic peak up to 1000°C. Above 1250°C, an exothermic peak appears which

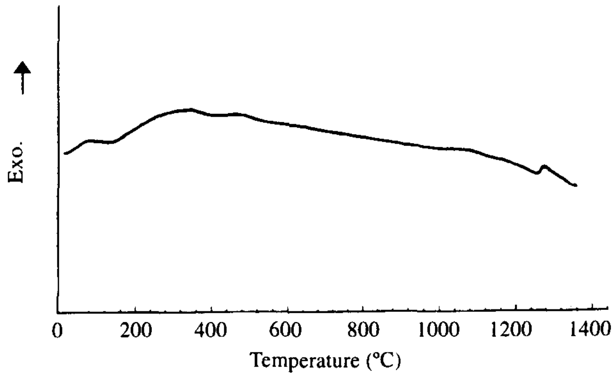

Fig. 2. DTA pattern of mullite precursor.

indicates the beginning of the crystallization of mullite. The X-ray diffraction (XRD) patterns of powders heated at 1000 and 1300°C are given in Fig. 3. XRD analysis confirmed that the precursor heated at 1000°C is essentially amorphous phase with minor quantities of Υ-Al_2O_3, whereas the precursor heated at 1300°C is crystalline mullite with no other crystalline phases. The xerogel prepared in this experiments is suitable to produce mullite whisker using the method described by Okada and Otsuka[18]

3.2 Mullite green compacts containing AlF_3 heat-treated in airtight condition

The most important factor of heat-treated process of mullite green compacts containing AlF_3 in airtight container is to choose a suitable temperature. After the treatment, a necessary amount of mullite whisker nuclei can be produce and the whisker cannot grow effectively, otherwise the whiskers could form a short network which could act as a barrier to densification. Synthesis of mullite whisker in F atmosphere carried out by means of vapor-phase reaction. For vapor-phase reaction, the fluorides must be volatilizable at the reaction temperature. F acts as a kind of catalyst because F does not exist in the final product—mullite whisker.

The formation reaction of mullite whisker may be as follows:[18]

$$6AlF_3 + 3O_2 \rightarrow 6AlOF + 12F \qquad (1)$$

$$Al_2O_3 + 2F \rightarrow 2AlOF + {}^1/_2O_2 \qquad (2)$$

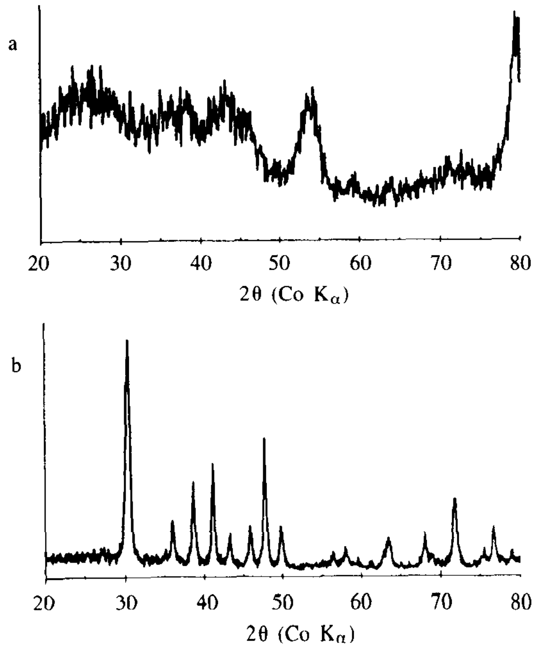

Fig. 3. X-ray diffraction patterns of mullite (precursor): (a) calcined at 1000°C; (b) calcined at 1300°C.

$$2SiO_2 + 8F \rightarrow 2SiF_4 + 2O_2 \qquad (3)$$

$$6AlOF + 2SiF_4 + 7/2O_2 \rightarrow 3Al_2O_3 \cdot 2SiO_2 + 14F \qquad (4)$$

The sublimation temperature of AlF_3 is at around 1040°C,[19] so the heat-treated temperature must be above 1040°C. In this experiment, the heat-treated temperature range is from 1100 to 1450°C in airtight condition for 4 h.

The sample treated at 1100°C, there is not any mullite peak existing, amorphous phase is the dominated phase [Fig. 4(a)]. After treated at 1150°C, results indicated that although a significant amount of amorphous phase still existed, mullite peaks have appeared obviously, as shown in Fig. 4(b). AlOF and SiF_4 were produced by adding AlF_3 and reacted each other to form mullite. Through this procedure, the mullitization temperature of the precursor prepared by hydrolysis–precipitation method is decreased intensively. In order to produce mullite whisker nuclei, it is necessary to treat the samples above 1150°C.

The SEM micrographs of fracture surfaces of mullite green compacts after treatment are shown in Fig. 5. There are no mullite whisker nuclei in the sample treated at 1100°C. The SEM micrograph of surface shows that the sample is composed of particles with a size below 0·1 μm in diameter [Fig. 5(a)]. After treatment at 1150°C, notable changes have taken place in fracture surface [Fig. 5(b)] due to the formation of mullite whisker nuclei. Above 1200°C, the changes are much great [Fig. 5(c)]. Further increasing the treating temperature up to 1400°C, a large amount of mullite whisker nuclei was formed as shown in Fig. 5(d)

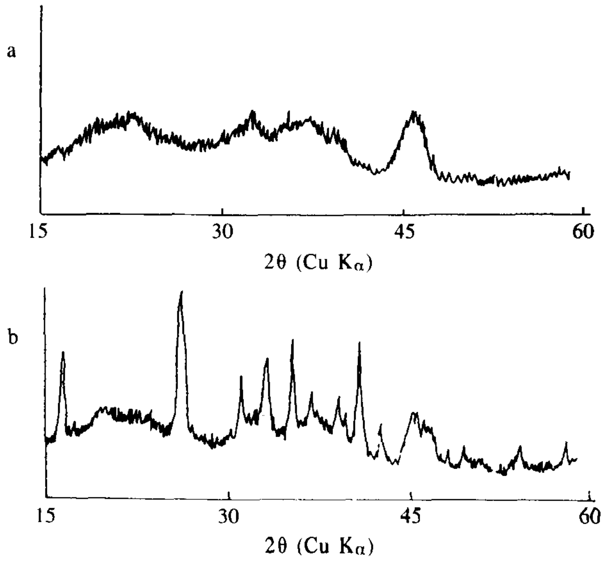

Fig. 4. XRD patterns of mullite samples: (a) 1000°C for 4 h; (b) 1150°C for 4 h.

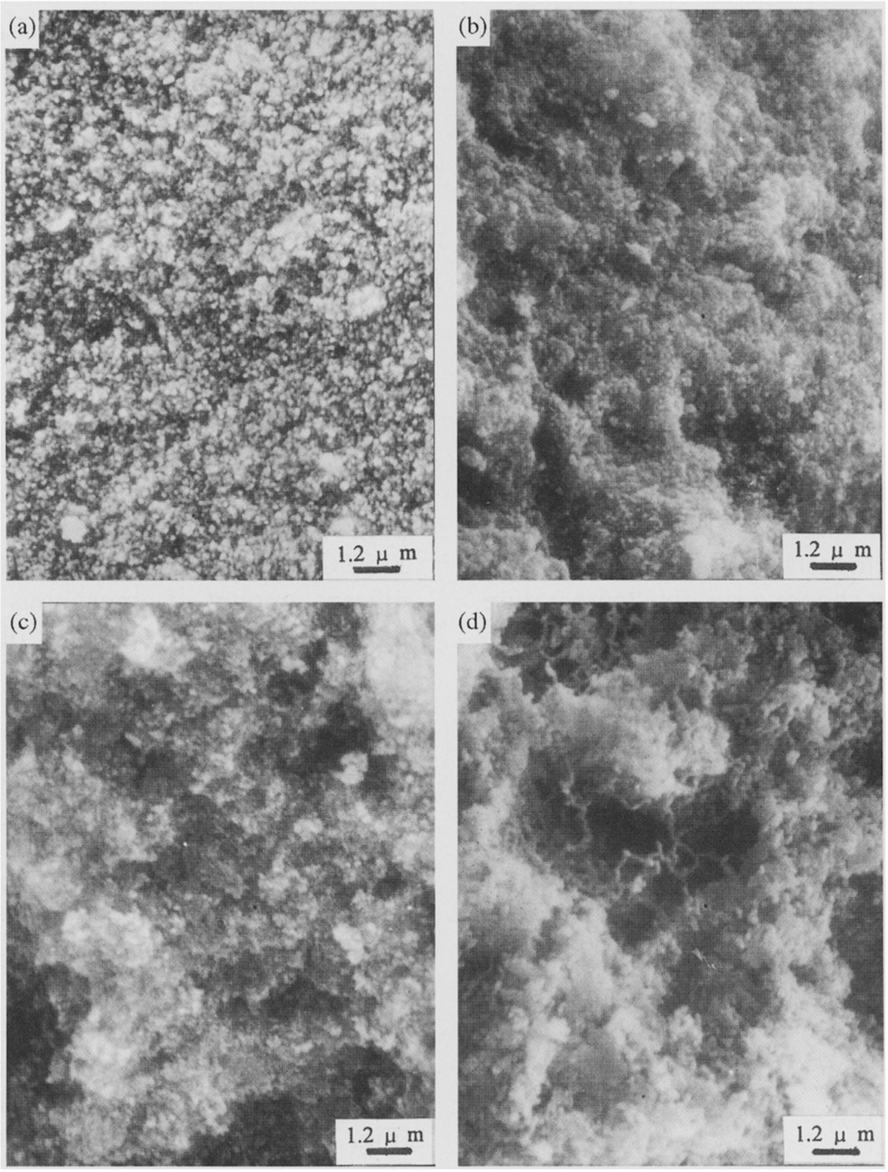

Fig. 5. SEM micrographs of fracture surfaces of mullite green compacts containing AlF_3 treated at various temperatures: (a) 1100°C for 4 h; (b) 1150°C for 4 h; (c) 1200°C for 4 h; (d) 1400°C for 4 h.

and some interlinked network of whisker can be observed in some parts.

3.3 Sintering and microstructure of mullite samples containing AlF_3 after heat-treatment

Densities of green compacts heat-treated at 1150 and 1200°C, respectively, in an airtight container are listed in Table 1. Sample 1 exhibits a higher density due to the precursor having a higher activity while sample 2 shows a nearly constant density because most of the precursor was calcined at 1250°C.

The dependence of the final relative density on sintering temperature is shown in Fig. 6. For sample 2 heat-treated at 1150°C, it can be observed that the relative density of sample increases with the increasing of the sintering temperature. The optimum relative density reached 97·6% at 1580°C for 4 h and then decreased with increasing the temperature up to 1600°C. Sample 1 heat-treated at 1150°C, the sintering curve exhibits a tendency similar to that of sample 2. At 1550°C for 4 h, the relative density is 98·3%. But those compacts heat-treated at 1200°C sintered at the same sintering conditions appeared much lower densities [< 90%, shown in Fig. 6(b)] because of the retarded forces existing in the samples. The relative density of

Table 1. Relative shrinkages and densities of samples at different heat treatment temperatures

Sample	*Green density ($g\,cm^{-3}$)*	*1150°C 4 h*		*1200°C 4 h*	
		Shrinkage (%)	*Density ($g\,cm^{-3}$)*	*Shrinkage (%)*	*Density ($g\,cm^{-3}$)*
1	1·26	7·20	1·32	9·50	1·36
2	1·25	1·40	1·25	1·50	1·25

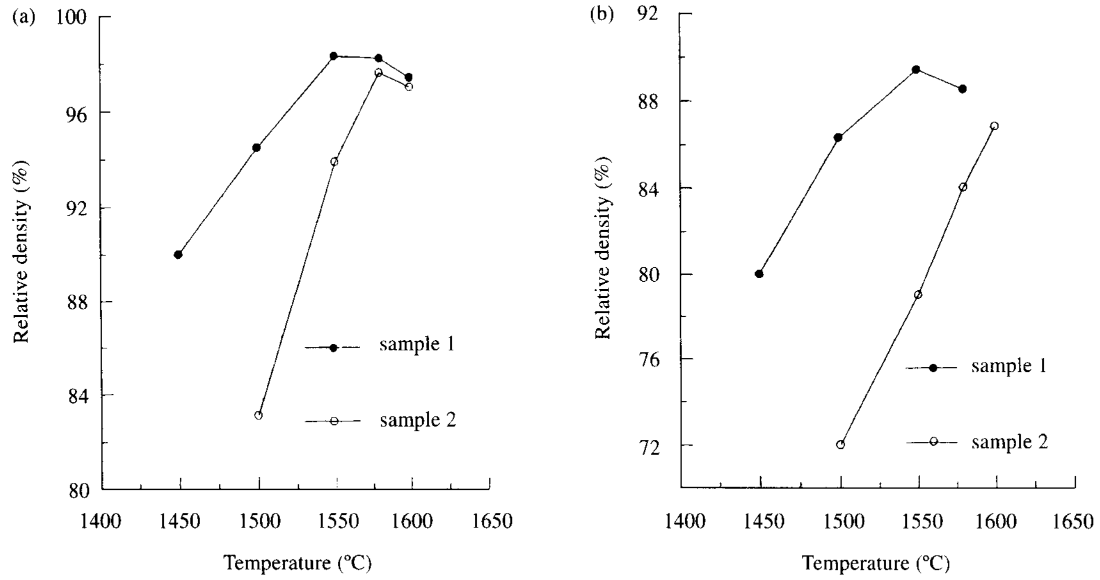

Fig. 6. The relationship of relative density and sintering temperature of samples after heat treatment in airtight condition: (a) 1150°C; (b) 1200°C.

sample 1 sintered at 1550°C was 89·4% and then decreased with increasing temperature. SEM of fracture surfaces of sample 2 (heat-treated at 1200°C and sintered at 1580°C for 4 h) shows that there are large pores with mullite whisker clumps about 0·1 μm in diameter existing in the matrix (Fig. 7). The whiskers could form a short network which acted as a barrier to densification. With increasing temperature, the mullite grains grew larger, but without shrinkages occurring to promote density. From above experiments, it can be concluded that heat treatment on compacts at 1150°C in an airtight container has no significant negative effects on densification. It is a relatively ideal treatment temperature.

As shown in Fig. 8, the microstructures which consist of equiaxed fine grains and rodlike mullite grains are quite similar to those of in-situ self-reinforcement Si_3N_4 ceramics.[9–11] Sample 1 sintered at 1550°C has a very fine equiaxed grains 0·1–0·3 μm in size and rodlike grains with high aspect ratio distributing uniformly in the matrix. The diameters of rodlike grains are significantly larger than those

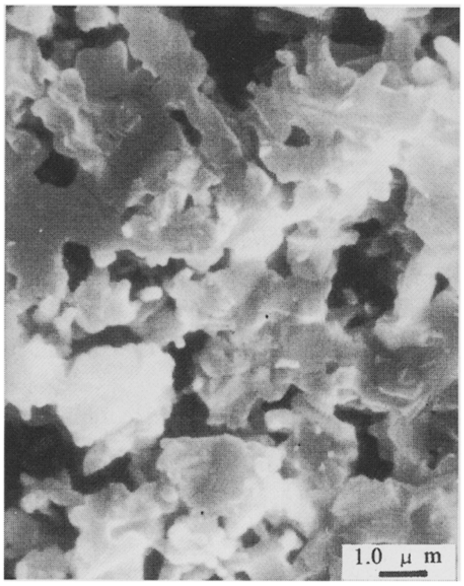

Fig. 7. SEM micrograph of fracture surfaces of sample 2 treated at 1200°C and sintered at 1580°C for 4 h.

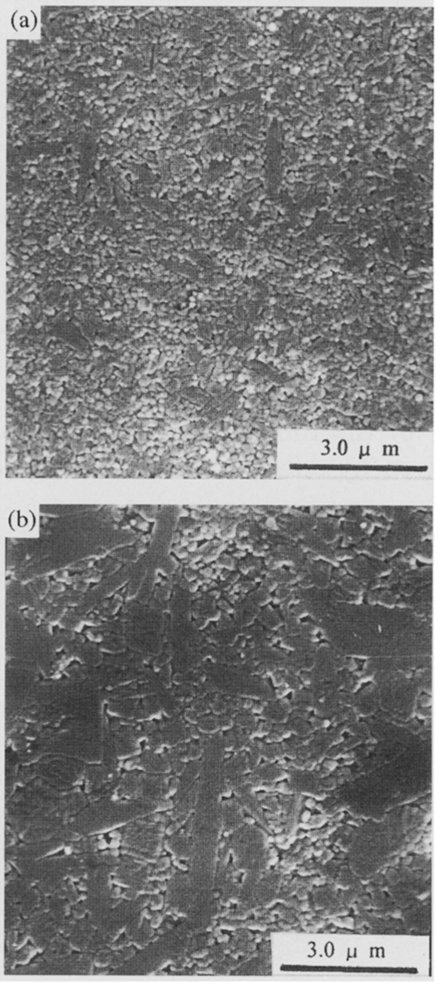

Fig. 8. SEM micrographs of mullite surfaces: (a) sample 1, 1550°C for 4 h; (b) sample 2, 1580°C for 4 h.

of equiaxed grains. The microstructure of sample 2 which is sintered at a higher temperature is characterized by rodlike mullite grains embedded in fine mullite grains about 0·2–0·6 μm in size [Fig. 8(b)]. In this structure, the rodlike grains grew more perfectly and no large defects left among them by forming network. The shapes of rodlike mullite grain are shown in Fig. 9. Similar morphology had been observed by Mohamed *et al.*[20] in their work by adding F into mullite precursor to produce mullite whisker. Compared with sample 1, sample 3 without the addition of AlF_3, as shown in Fig. 10(a), there are fewer rodlike mullite grains present in the sintered body and their growth is less perfectly than those of samples having AlF_3 [Fig. 10(b)]. Although the SiO_2-rich composition (68/32) which is associated with liquid phase forming during sintering makes rodlike grains grow easily,[12,13] rodlike grains did not increase with increasing the amount of liquid phase. Adding AlF_3 into mullite precursor and then heat treated the mixture at 1150°C. The Al_2O_3/SiO_2 ratios of materials were changed by the loss of mass and SiO_2 is slightly lower than that of the initial composition. It was confirmed by the data in Table 2. The results also explained the size differences of equiaxed grains between samples 1 and 3. The relatively lager grains in sample 3 were a result of the relatively larger volume of liquid phase. This fact implies that the volume of the liquid phase is not the only condition to control the growth of rodlike grains. In order to examine the chemical composition of rodlike grains, the Al_2O_3/SiO_2 ratio of four rodlike grains in sample 2 (sintered at 1580°C for 4 h) were measured by EDX using TEM. The number of measuring points was at least four for each selected grain and the average values are listed in Table 3. The results indicated that the Al_2O_3/SiO_2 ratio of the center part is much higher than that of the rim part. The phase-diagram of mullite given by Aksay and Pask[6] illustrated that the Al_2O_3/SiO_2 ratio of mullite would decrease with increasing sintering temperature below 1350°C. In this experiment, with the addition of AlF_3 into mullite precursor, the mullitization temperature decreased greatly. So the synthesed mullite has a higher Al_2O_3/SiO_2 ratio. Okada and Otsuka[21] also demonstrated that the Al_2O_3/SiO_2 ratio of mullite whisker decreased with increasing firing temperature in their research work. Mullite whisker nuclei with a high Al_2O_3/SiO_2 ratio produced during heat-treated procedure at 1150°C

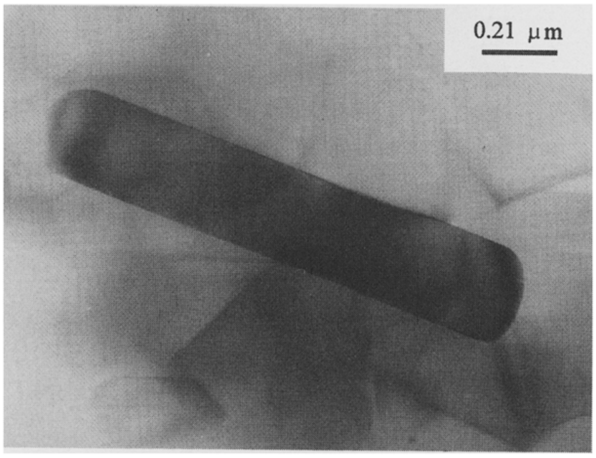

Fig. 9. TEM micrograph of rodlike mullite grain sample 2 treated at 1150°C and sintered at 1580°C for 4 h.

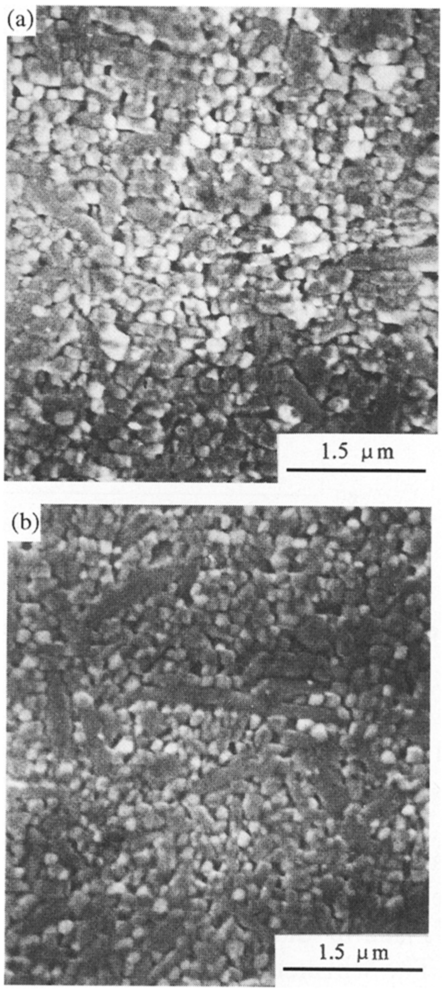

Fig. 10. SEM micrographs of mullite samples: (a) sample 3, 1550°C for 4 h; (b) sample 1, 1550°C for 4 h.

Table 2. EDX analysis results of samples 1 and 3

Sample	*Sintering condition*	*Al_2O_3/SiO_2 (wt/wt)*
1	1550°C 4 h	69·89/30·11
2	1550°C 4 h	68·22/31·78

Table 3. Al_2O_3/SiO_2 ratios of rodlike mullite particles

Grain	*Center Al_2O_3/SiO_2 (wt/wt)*	*Rim Al_2O_3/SiO_2 (wt/wt)*
1	75·1/24·9	69·2/30·8
2	75·3/24·7	70·9/29·1
3	75·5/24·5	69·8/30·2
4	74·9/25·1	68·9/31·1

were used as centers for nuclei growth during sintering and grew in the selected direction by choosing the Al_2O_3/SiO_2 ratio. In the case of grain growth accompanying liquid phase sintering, small particles dissolved in liquid phase and precipitated on large particles. The high Al_2O_3/SiO_2 is required to form rodlike grains.

From the above analysis, two necessary conditions for producing rodlike mullite were: (1) existence of high Al_2O_3/SiO_2 ratio grains; (2) existence of liquid phase which causes small grains dissolving and precipitation on large grains.

Table 4. Mechanical properties of mullite ceramics

Sample	*Sintering temperature (°C)*	*Flexural strength (MPa)*	*Fracture toughness (MPa $m^{1/2}$)*
3	1550	250 ± 40	1·94 ± 0·34
1	1550	280 ± 32	2·48 ± 0·22
2	1580	265 ± 52	2·97 ± 0·37

3.4 Flexural strength and fracture toughness

As shown in Table 4, the fracture toughness of sample 1 (1550°C sintered) and sample 2 (1580°C sintered) increased by the growth of rodlike mullite grains and flexural strength did not decrease. This indicated that the growth of rodlike grains could not lead to large defects among matrix which can be seen in Fig. 8. Compared with sample 3, the fracture toughness of samples 1 and 2 increased 27·8 and 53·1%, respectively.

The fracture surface of sample 3 in Fig. 11(a) was relatively flat and showed mainly transgranular fracture. However, the rough and complex features are observed on the fracture surface of sample 1 and rodlike particles pulling out from matrix are also observed, as shown in Fig. 11(b) and (c). It demonstrated that the growth of rodlike particles changed the fracture mode from mainly transgranular to the mixture type of transgranular and intergranular in monphase mullite ceramics. The area of fracture increased and it could absorb much more energy. Therefore the growth of rodlike mullite increased the toughness of mullite ceramics.

Fig. 11. SEM micrographs of fracture surfaces of samples: (a) sample 3, 1550°C; (b) and (c) sample 1, 1550°C.

4 Conclusion

1. A new experiment route was designed to fabricate rodlike mullite particles among equiaxed grain matrix: AlF_3 was added into mullite precursor and then heat treated in airtight condition. During this process, mullite whisker nuclei were formed and could be used as growth centers for rodlike grains.
2. The experiment results demonstrated that 1150°C was a proper heat-treated temperature for mullite precursor with the addition of AlF_3. Above 1150°C, densification bodies could not be obtained after the following sintering process.
3. The necessary conditions for rodlike grain growth were existence of high ratio composition gains and existence of liquid phase. In this experiment, after sintered at higher tem-

perature, mullite/mullite (rodlike) microstructure was obtained for the samples containing AlF_3 heat-treated at 1150°C in airtight condition.

4. The growth of rodlike particles improved the fracture toughness of matrix and did not decrease the flexural strength.

References

1. Aksay, I. A., Dabbs, D. M. and Sarikaya, M., Mullite for structural, electronic, and optical application. *J. Am. Ceram. Soc.*, 1991, **74**(10), 2343–2358.
2. Kanzaki, S., Tabata, H., Kumazawa, T. and Ohta, S., Sintering and mechanical properties of stoichmiometric mullite. *J. Am. Ceram. Soc.*, 1985, **68**(1), C6.
3. Dokko, P. C., Pack, J. A. and Mazdiyasni, K. S., High-temperature mechanical of mullite under compression. *J. Am. Ceram. Soc.*, 1977, **60**(3–4), 150–155.
4. Schneider, H. and Eberhand, E., Thermal expansion of mullite. *J. Am. Ceram. Soc.*, 1990, **73**(7), 2073–2076.
5. Dovis, R. F. and Posk, J. A., Diffusion and reaction studies in the system Al_2O_3–SiO_2. *J. Am. Ceram. Soc.*, 1972, **5**(10), 525–531.
6. Aksay, I. A. and Pask, J. A., Stable and metastable equilibria in the system SiO_2–Al_2O_3. *J. Am. Ceram. Soc.*, 1975, **58**(11–12), 507–512.
7. Hori, S., Kaji, H., Yashimura, M. and Somiya, S., Deflection-toughened comundum-rutile composites. *Mater. Res. Soc. Symp. Proc.*, 1987, **78**, 283–288.
8. Lee, D. D., Kang, S. J. L. and Yoon, D. N., Mechanism of grain growth and α–β transformation during liquid-phase sintering of β-sialon. *J. Am. Ceram. Soc.*, 1988, **79**(1), 803–806.
9. Mitomo, M. and Uenosono, S., Microstructural development during gas-pressure sintering of α-silicon nitride. *J. Am. Ceram. Soc.*, 1992, **75**(1), 103–108.
10. Mitomo, M. and Mizuno, K., Sintering behaving of Si_3N_4 with Y_2O_3 and Al_2O_3 addition. *Yogyo Kyokaishi.*, 1986, **94**(1), 96–101.
11. Tani, E., Umebayashi, S., Kishi, K., Kobayashi, K. and Nishijima, N., Gas-pressure sintering of Si_3N_4 with concurrent addition of Al_2O_3 and 5 wt% rare earth oxide: high fracture toughness Si_3N_4 with fiber-like structure. *Am. Ceram. Soc. Bull.*, 1986, **65**(9), 1311–1315.
12. Kumazama, T., Kanaki, S. and Ohta, S., Influence of chemical composition on the mechanical properties of SiO_2–Al_2O_3 ceramic. *J. Ceram. Soc. Jpn (inter. ed.)*., 1988, **96**(2), 85–91.
13. Kumazawa, T., Kanaki, S., Asaumi, J., Abe, O. and Tabata, H., Sinter ability of SiO_2–Al_2O_3 powers prepared by spray pyrolysis. *Yogyo Kyokais.*, 1986, **94**(5), 485–490.
14. Schneider, H. Okada, K. and Pask, J., *Mullite and Mullite Ceramics.* John Wiley and Sons, Chichester, UK, 1994.
15. Deer, W., Howie, R. A. and Zussman, J. (eds), Rock-forming minerals, Vol. 1A (second edition), Geological Society Publishing House, Bath, UK, 1997.
16. Somiya, S. and Hirata, Y., Mullite powder technology and applications in Japan. *Am. Soc. Ceram. Bull.*, 1991, **70**(10), 1624–1632.
17. Xu, M. X., Cui, F. and Jing, Z. G., Study on preparation of ultra-fine mullite powder. *J. Chin. Ceram. Soc.*, 1991, **19**(1), 80–85.
18. Okada, K. and Otsuka, N., Synthesis of mullite whisker by vapour-phase reaction. *J. Mater. Soc. Lett.*, 1989, **8**(9), 1052–1054.
19. Japan Chemical Society (eds), *Handbook of Chemistry*, Vol. 1. Maruzen Co. Ltd., Tokyo, Japan, 1966.
20. Mohamed, G., Ismail, M. U., Hiroshi, A., Zenjira, N. and Tokuji, A., Mullite whiskers from precursor gel powders. *J. Am. Ceram. Soc.*, 1990, **73**(9), 2736–2739.
21. Okada, K. and Otuska, N., Synthesis of mullite whisker and their application in composites. *J. Am. Ceram. Soc.*, 1991, **74**(10), 2414–2418.